EUROPEAN ORGANIZATION FOR NUCLEAR RESEARCH

CERN-EP/85-44
3 April 1985

OBSERVATION OF DOUBLE-POMERON EXCHANGE IN ALPHA-ALPHA COLLISIONS AT THE CERN INTERSECTING STORAGE RINGS

V. Cavasinni, T. Del Prete, M. Morganti and F. Schiavo
Dipartimento di Fisica dell'Università and INFN, Pisa, Italy

D. Lloyd Owen[1)]
CERN, Geneva, Switzerland

G. Paternoster and S. Patricelli
Dipartimento di Fisica dell'Università and INFN, Naples, Italy

G. Anzivino[2)]
State University of New York, Stony Brook, NY, USA

ABSTRACT

We observed the process $\alpha\alpha \to \alpha\alpha X$ in which the α's were emitted uncorrelated in the forward direction and the charged component of the cluster X was confined to a limited portion ($|\eta| \lesssim 2$) of the central region. We identified such reactions as being due to double-Pomeron exchange, for which we found a cross-section of (720 ± 140) μb. The raw mean charged multiplicity of the cluster X was found to be 6.76 ± 0.07 with a dispersion D = 4.8. The measurements were performed at the CERN ISR at a centre-of-mass energy of $\sqrt{s}$ = 126 GeV. Similarities are drawn between double-Pomeron exchange in $\alpha\alpha$ and in pp collisions.

(Submitted to Zeitschrift für Physik C)

---

1) Present address: State University of New York, Stony Brook, NY, USA.
2) Present address: CERN, Geneva, Switzerland.

1. INTRODUCTION

Double-Pomeron exchange (DPE) was originally formulated in the framework of the Regge model [1-3], and was investigated experimentally as a means of elucidating the properties of that complicated object: the Pomeron. More recently, interest in DPE has been revived by a possible interpretation of the Pomeron as a multi-gluon state [4]. In this context it has been suggested that DPE might be a good mechanism for producing gluonium [5].

Experimentally most of the data came from the ISR, where DPE was measured in proton-proton interactions [6-8]. The major concern in these experiments was to isolate genuine DPE events from processes involving reggeon (ρ and ω) exchange and from single diffraction events which could match the rapidity distribution expected for DPE.

In this paper, we present the results of an investigation of DPE in $\alpha\alpha$ collisions at the CERN Intersecting Storage Rings (ISR). The experimental signature of such a process is simple: the incident particles emerge from the interaction in the forward direction and are uncorrelated in angle; they are accompanied by a low-mass cluster at rapidity ≈ 0. In alpha-alpha interactions the isolation of DPE processes is simpler than the proton-proton ones since the non-DPE background is more restricted. Competing exchanges (e.g. ρ and ω) are forbidden because the α has both spin and isospin 0, and diffraction excitation leads to the disintegration of the α's.

In the following sections we first discuss the experimental apparatus and the analysis. We then present the results of the measurement: the DPE cross-section and some properties associated with the accompanying central cluster.

2. EXPERIMENTAL APPARATUS

The apparatus was primarily designed for the measurement of total and elastic interaction cross-sections, and is described in greater detail elsewhere [9,10]. It consisted of sets of scintillation-counter hodoscopes that together covered virtually the entire solid angle. The left- and right-arm telescopes were mirror images of each other, and coverage in each arm was provided by five hodoscopes:

CIO ($0 < \eta < 1.5$), H12 ($1.2 < \eta < 3.0$), H34 ($2.5 < \eta < 4.5$), H5 ($4 < \eta < 5$), and TB ($4.5 < \eta < 6$). Each hodoscope was equipped to measure the polar angles of charged secondaries with coarse definition of their azimuthal angles.

The scintillation counters were complemented in the central region ($|\eta| < 2.0$) by a drift-chamber vertex detector [11].

The α's were detected by telescopes located symmetrically at 9.2 m from the intersection point. Each telescope comprised (Fig. 1):

- Two planes of scintillation counters (TB_A and TB_B) which provided the α trigger. The pulse height (PH) of each individual counter was also recorded to provide specific ionization measurement for off-line analysis.
- Two arrays of 9 'finger' scintillators (TB_y), each 25×90 mm^2. The arrays consisted of two planes staggered horizontally by 12.5 mm.
- Two arrays of drift tubes (DT) [12], each array consisting of two planes of 12 tubes staggered vertically to resolve up/down ambiguities. The tube was a cylinder 10 mm in diameter and 300 mm in length, with 250 μm aluminium walls and a 40 μm sense wire along the cylindrical axis.

The trigger used to select candidate DPE events was:

$$T = (TB * \overline{H34} * CIO)_{left} * (CIO * \overline{H34} * TB)_{right} ,$$

i.e. the trigger required hits at small angle in both arms in coincidence with hit(s) in the central region, with a pseudorapidity gap of 2 units between the small- and wide-angle tracks.

A total of 100,000 events were collected in August 1983. The currents circulating in the ISR were $I_1 = 4.5$ A and $I_2 = 5.3$ A. The ISR luminosity during data acquisition was monitored by the $H_{34}^{Right} * H_{34}^{Left}$ coincidence rate, and found to be 0.81×10^{29} cm^{-2} sec^{-1}. The $H_{34}^{Left} * H_{34}^{Right}$ monitor cross-section, 174 ± 9 mb, was calibrated using the van der Meer method [13,14]. With this luminosity (and excellent single-beam background) the number of events rejected because of accidental signals in H_{34} was found to be 0.8%.

3. ANALYSIS

The forward α's were identified off-line through their specific ionization in the TB counters. A scatter plot of events versus the pulse heights measured in the two arms reveals the expected four peaks: singly charged tracks in both arms (normal inelastic events); a singly charged track in one arm and a doubly charged track in the other (single diffractive events); and doubly charged tracks in both arms (DPE candidate events). There are no evident peaks corresponding to a single counter detecting two singly charged tracks.

The candidate DPE sample was selected by imposing the cuts shown in Fig. 2. This reduced the event sample to 6738 events. The contamination of this sample from the tails of the other peaks was determined by extrapolating the distribution of events in B and C underneath A and it was estimated to be < 5%.

The identification of α's on the basis of ionization measurements has a shortcoming in that no distinction is made between an α and a ^{3}He. This, coupled with the fact that the process

$$\alpha\alpha \rightarrow \alpha\, ^3\mathrm{He}\, X$$

can proceed via the exchange of something other than a Pomeron, could lead to the misidentification of a non-DPE process as a DPE reaction.

One mechanism whereby a ^{3}He can be produced is the diffractive excitation of an α followed by the decay: $\alpha^* \rightarrow {}^3\mathrm{He} + n$. The contamination of the event sample via this mechanism would have been the same as in the parallel channel in which the excited α decays into ^{3}H + p. Owing to the small energy available in the decay (about 20 MeV), the proton and the tritium would be well collimated along the direction of the α^* and both would be detected by the TB counters in a large fraction of cases. (Evidence for this process has indeed been given in a previous paper [15], where it represented a serious background to the elastic cross-section measurements). The absence of a two-singly-ionizing-particle peak in Fig. 2 argues against a significant contribution from either process.

A similar source of misidentification could have arisen through a collision in which two of the constituent neutrons of the α's interact, yielding fragments

only in a narrow central region, while the spectator ^{3}He suffer little perturbation. Our argument against contamination from this source is based on the topology of the central cluster: the nn scattering must resemble pp or $p\bar{p}$ scattering at the same energy per nucleon, and a parallel analysis of such events, which imposed this restrictive topology off-line, indicated this to be sufficiently rare that the contribution in $\alpha\alpha$ be insignificant.

The resolution that could be obtained in the measurement of α scattering angles was limited by the finite dimensions of the beam-crossing region. Angular cells were thus defined by the overlap of drift-tube and scintillation-counter cells (5 mm by 12.5 mm), which gave an angular resolution comparable to the limit set by the extent of the source. The mean polar angle of the tracks detected by each cell was calculated by a Monte Carlo which took the size of the source into account. This angle was then used to estimate the momentum transfer t imparted to the scattered α's:

$$t = p_{ISR}^2 \left[\cos(\theta_\alpha) - 1 \right] ,$$

where we assumed that each α retained the full beam momentum, as would be the case for DPE. Figure 3 is a scatter plot of the momentum transfer measured for the two α's.

A potential source of background to the measurement was the pile-up of an inelastic and an elastic event. We calculated that the contamination of the sample arising from such a background was < 1%. This result is confirmed by the lack of an accumulation of events along the diagonal of the scatter plot.

The production of δ-rays upstream from the elastic detector lead to spurious hits in cells other than those containing the triggering track in about 30% of the candidate sample. Such events were rejected from the sample, and taken into account later by applying a correction factor to the resulting cross-section.

This correction factor was calculated assuming that all the events which passed the pulse-height cut and which had at least a track on each TB telescope were DPE events.

The charged particles of the central cluster X were detected by CIO and H12, and, over a more limited polar region, by the drift chambers. These detectors were subject to instrumental effects (secondary interactions, photon conversion, finite counter size, etc.) that complicated the measurement of absolute quantities. Since our aim in the present work is only the comparison of multiplicities for different categories of events, we did not attempt to correct the raw distributions for such effects.

4. RESULTS

4.1 The DPE cross-section

Since the upper and lower vertices of the DPE diagram (Fig. 4) factorize, the doubly differential scattering cross-section may be expressed as*):

$$\frac{d^2\sigma}{dt_L dt_R} = A\, f(t_L) f(t_R) \ ,$$

which may then be integrated to obtain the singly differential form:

$$\frac{d\sigma}{dt} = A'\, f(t) \ ,$$

where t refers to either of the α's. This cross-section is presented in Fig. 5. The errors in the figure are statistical only; contributions to systematic errors arise from:

a) uncertainty (±10%) in the correction factor applied to account for events with δ-rays that were removed from the sample;

b) uncertainty (±10%) in solid angle (mainly due to finite source size); and

c) uncertainty (±5%) in the overall normalization (reflecting the uncertainty in the luminosity calibration).

The resolution in t was ±0.02 GeV^2, and was determined principally by the width of the TB scintillator elements. As the figure shows, the data are well represented

*) The study of azimuthal correlations between the α's was hampered by the non-uniform acceptance of our detector (Fig. 1) and by the strong dependence of the cross-section on polar angle. The equality of rates when the difference of the α's azimuthal angle was 0 or π argues against any significant effect.

by an exponential in t [f(t) = exp (bt)], and the curve is the fit obtained under this assumption. The fitted parameters have the values:

$$A' = (8.8 \pm 1.7)\ \text{mb/GeV}^2$$

$$b = (12.2 \pm 0.3)/\text{GeV}^2 ,$$

where systematic errors have been combined with statistical ones. The χ^2/NDF of the fit was 42/30.

In an earlier work [15] we showed that the differential cross-section for elastic $\alpha\alpha$ scattering could be parametrized as the sum of two interfering exponentials in t. In the t region of the present measurement, the elastic slope has the value b(el) = $(23.8 \pm 0.5)/\text{GeV}^2$; so, forming the ratio, we obtain:

$$\frac{b(\text{DPE})}{b(\text{el})} = 0.51 \pm 0.03$$

consistent with the value of ½ expected through the assumption of factorization (see Ref. [8]).

Integrating the exponential form, we obtain the total DPE cross-section:

$$\sigma_{\text{tot}}(\text{DPE}) = (720 \pm 140)\ \mu\text{b} ,$$

where statistical and systematic errors have again been combined.

In order to compare our $\alpha\alpha$ DPE measurement with the pp DPE measurements of Drijard et al. [8], we repeated our analysis imposing the same topological constraints on events as these authors, i.e. two α's at small angles, two charged tracks in the region $|\eta| < 1$, and no charged tracks elsewhere. The more restrictive cuts in η did not affect the shape of $d\sigma/dt$ appreciably, but reduced the normalization by about a factor of 5:

$$\sigma_{\text{tot}}^{\eta<1}(\alpha\alpha;\ \text{DPE}) = (131 \pm 25)\ \mu\text{b} ,$$

(of which 45% of the cross-section corresponds to two tracks in the central cluster). This is to be compared with

$$\sigma_{\text{tot}}^{\eta<1}(\text{pp};\ \text{DPE}) = (11.7 \pm 3.0)\ \mu\text{b} .$$

Comparing the ratio of total DPE and total interaction cross-sections in $\alpha\alpha$ and pp collisions at $\sqrt{s}$ = 126 and 63 GeV, respectively, we obtain

$$R(\alpha\alpha;\ \text{DPE/total}) = (0.20 \pm 0.06) \times 10^{-3}$$

$$R(pp;\ \text{DPE/total}) = (0.27 \pm 0.07) \times 10^{-3}$$

Within errors, the ratio is the same for the different initial states and the different incident energies.

4.2 The central cluster

In this section, we illustrate some of the properties of the central cluster through a comparison of the DPE sample (sample A) with two other categories of events. Sample B contained events matching the DPE trigger, but with the requirement that the small-angle tracks were NOT α's: these events filled region C in Fig. 2.

Sample C contained inelastic pp events with the same topological requirements as in the other two samples at $\sqrt{s}$ = 31 GeV (i.e. the same energy per nucleon as in the $\alpha\alpha$ case). This latter sample will simulate the neutron-neutron interactions that could contaminate the DPE events as discussed above.

In Figs. 6a-c we present the uncorrected cluster multiplicity distributions for the three samples. The data in the figures correspond to tracks reconstructed in the vertex detector, and have been normalized so that each figure contains the same number of events, noting in each case the mean charged multiplicity and its dispersion. As inspection shows, the cluster multiplicity in DPE events is significantly lower (by about 30%) than in normal elastic events with similar topology.

We calculate the dispersion in η of the tracks in the events for the three samples, both inclusively and semi-inclusively (i.e. for fixed ranges of charged multiplicity). The results for the mean value of the dispersion are listed in Table 1.

In the low-multiplicity ranges, where the DPE events are concentrated, the dispersion in η is smaller for the DPE sample than for the other two; in the higher-multiplicity ranges the three samples are broadly similar. The comparison shows that, as expected in DPE, the central cluster has lower multiplicity and is more collimated in rapidity than in normal inelastic interactions.

We can further use the data on multiplicity to assess an upper limit on the non-DPE contamination in the DPE sample. Assuming that the DPE candidate events at high multiplicity ($n > 15$) are solely due to neutron-neutron scattering within the α's and that the topology of such events is the same as that of pp events at the same c.m. energy per nucleon (sample C), we normalized the sample-C multiplicity distribution to the tail of the sample-A distribution. The result is the broken line in Fig. 6a. Integrating, we placed an upper limit of 30% for contamination from this source.

5. CONCLUSIONS

We searched for interactions proceeding via DPE in $\alpha\alpha$ collisions at $\sqrt{s}$ = = 126 GeV. A fraction of these collisions, corresponding to a cross-section of (720 ± 120) μb, satisfied topological criteria and could thus be identified as DPE. This fraction is the same as that found in pp collisions at $\sqrt{s}$ = 63 GeV.

Acknowledgements

The advice and assistance of G. Carboni, P.D. Grannis and M. Valdata-Nappi at all stages of the experiment are warmly appreciated. We are also indebted to M. Ambrosio and G.C. Barbarino for their contribution at an early stage of the experiment. The technical assistance of G.C. Barnini, A. Bechini and L. Giacomelli is gratefully acknowledged. We also wish to thank Mrs R. Dubos-Latrauguere for the administrative assistance she has provided.

REFERENCES

[1] R. Shankar, Nucl. Phys. B70 (1974) 168.

[2] A.B. Kaidalov and K.A. Martirosyan, Nucl. Phys. B75 (1974) 422.

[3] D.P. Roy and G.G. Roberts, Nucl. Phys. B82 (1974) 471.

[4] See, for example, A. Donnachie and P.V. Landshoff, Phys. Lett. 123B (1983) 345.

[5] D. Robson, Nucl. Phys. B130 (1977) 328.

[6] M. Della Negra et al., Phys. Lett. 65B (1976) 394.

[7] L. Backsay et al., Phys. Lett. 68B (1977) 385.

[8] D. Drijard et al., Nucl. Phys. B143 (1978) 61.

[9] G. Carboni et al., Phys. Lett. 108B (1982) 145.

[10] M. Ambrosio et al., Phys. Lett. 115B (1982) 495.

[11] A. Bechini et al., Nucl. Instrum. Methods 156 (1978) 181.

[12] U. Becker et al., Nucl. Instrum. Methods 180 (1981) 161.

[13] S. van der Meer, CERN Internal Report ISR-PO/68-31 (1968).

[14] G. Carboni et al., preprint CERN-EP/84-163, 29 November 1984, to appear in Nucl. Phys. B.

[15] M. Ambrosio et al., Phys. Lett. 113B (1982) 347.

Table 1

Average dispersion ($\bar{\Delta}$) in pseudorapidity of the cluster X for the three samples of events and as a function of the charged multiplicity. The table shows also the percentage of events of each subsample relative to the total.

Multiplicity	αα DPE (sample A)		αα inelastic (sample B)		pp inelastic (sample C)	
	$\bar{\Delta}$	% of total	$\bar{\Delta}$	% of total	$\bar{\Delta}$	% of total
any	0.71 ± 0.01	100	0.85 ± 0.01	100	0.89 ± 0.01	100
2-3	0.52 ± 0.01	29	0.58 ± 0.01	13	0.59 ± 0.03	6
4-6	0.73 ± 0.01	32	0.80 ± 0.01	27	0.85 ± 0.02	20
7-10	0.84 ± 0.01	22	0.89 ± 0.01	26	0.92 ± 0.01	29
11-15	0.90 ± 0.01	11	0.93 ± 0.01	18	0.97 ± 0.01	25
16-20	0.94 ± 0.01	4	0.95 ± 0.01	9	0.97 ± 0.01	14
21-25	0.97 ± 0.02	1	0.96 ± 0.01	4	0.95 ± 0.01	4
26	0.97 ± 0.02	1	0.96 ± 0.01	3	0.94 ± 0.02	2

Figure captions

Fig. 1 : The TB telescope. TB_A and TB_B are trigger counters. TB_y is a hodoscope of two staggered 'finger' scintillators and TB_z consists of two staggered planes of drift tubes.

Fig. 2 : Scatter plot of the pulse height of the TB_L versus the TB_R.

Fig. 3 : Scatter plot of t_L versus t_R for events populating region A in Fig. 2.

Fig. 4 : Double Pomeron Exchange (DPE) diagram for $\alpha\alpha \to \alpha\alpha X$.

Fig. 5 : Distribution of the α momentum transfer squared for DPE events. The solid line is a fit described in the text.

Fig. 6 : Raw multiplicity distribution for a) $\alpha\alpha$ DPE events, b) $\alpha\alpha$ inelastic events, and c) pp inelastic events (see the text). The three distributions are normalized to the same area. The broken line in Fig. 6a is the distribution of Fig. 6c normalized to the tail of Fig. 6a ($n > 15$).

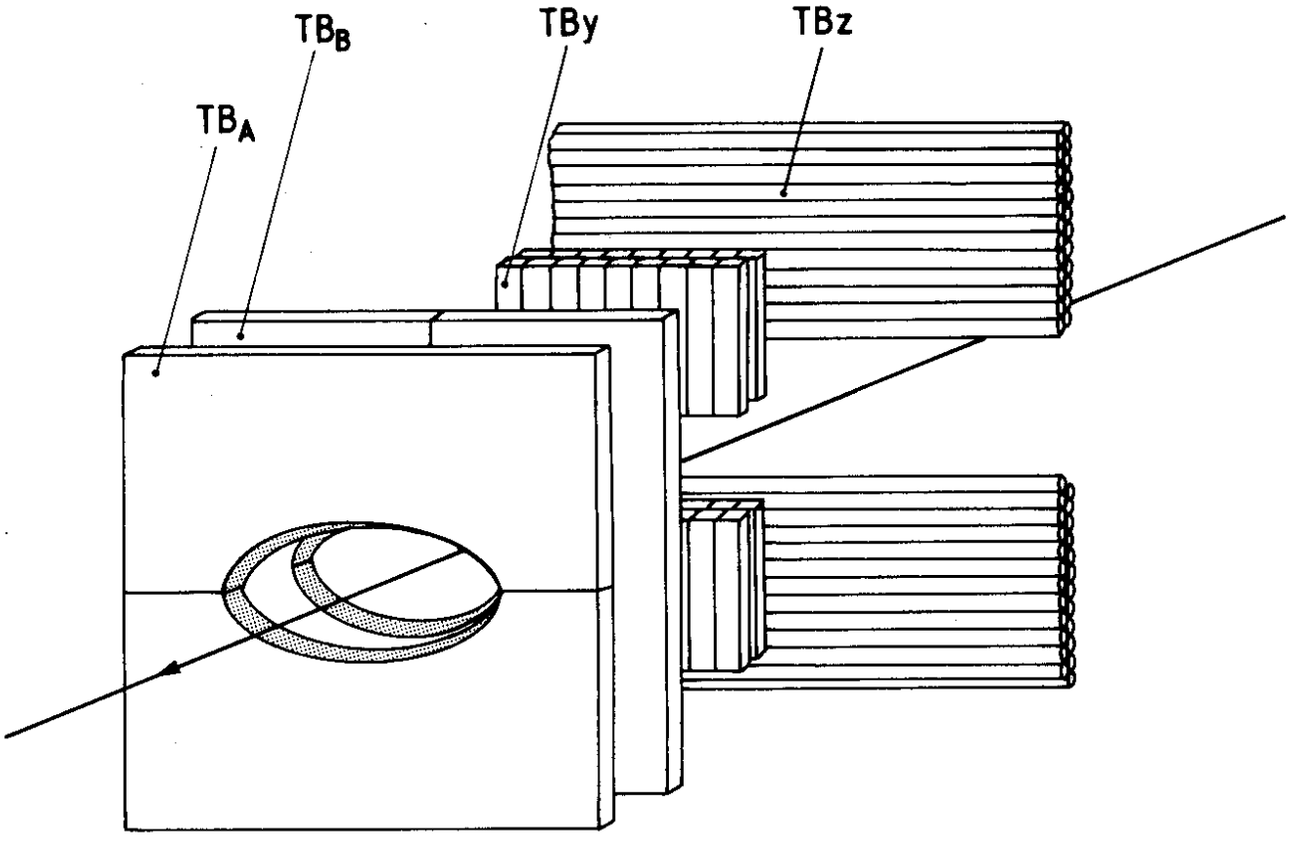

Fig. 1

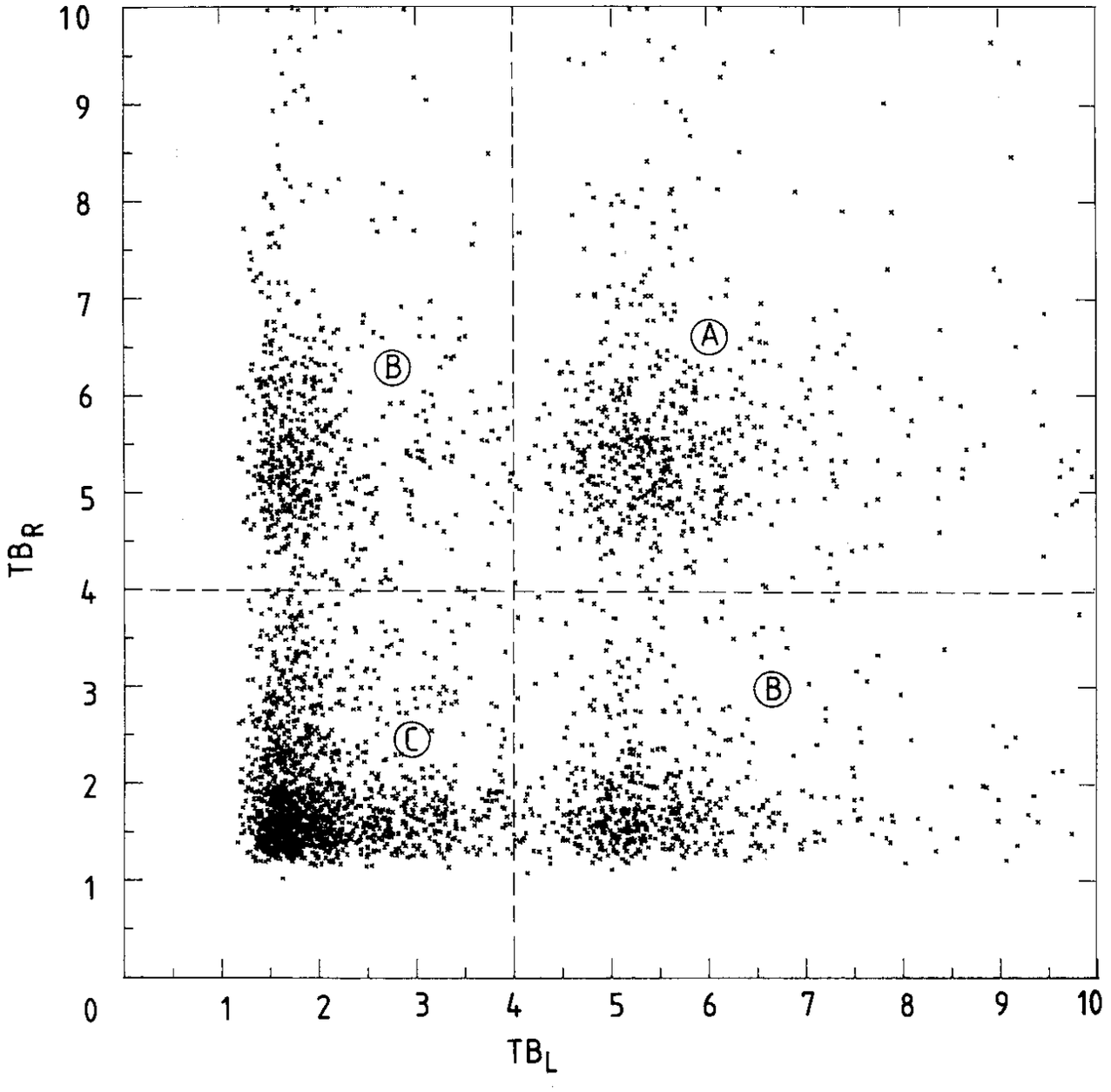

Fig. 2

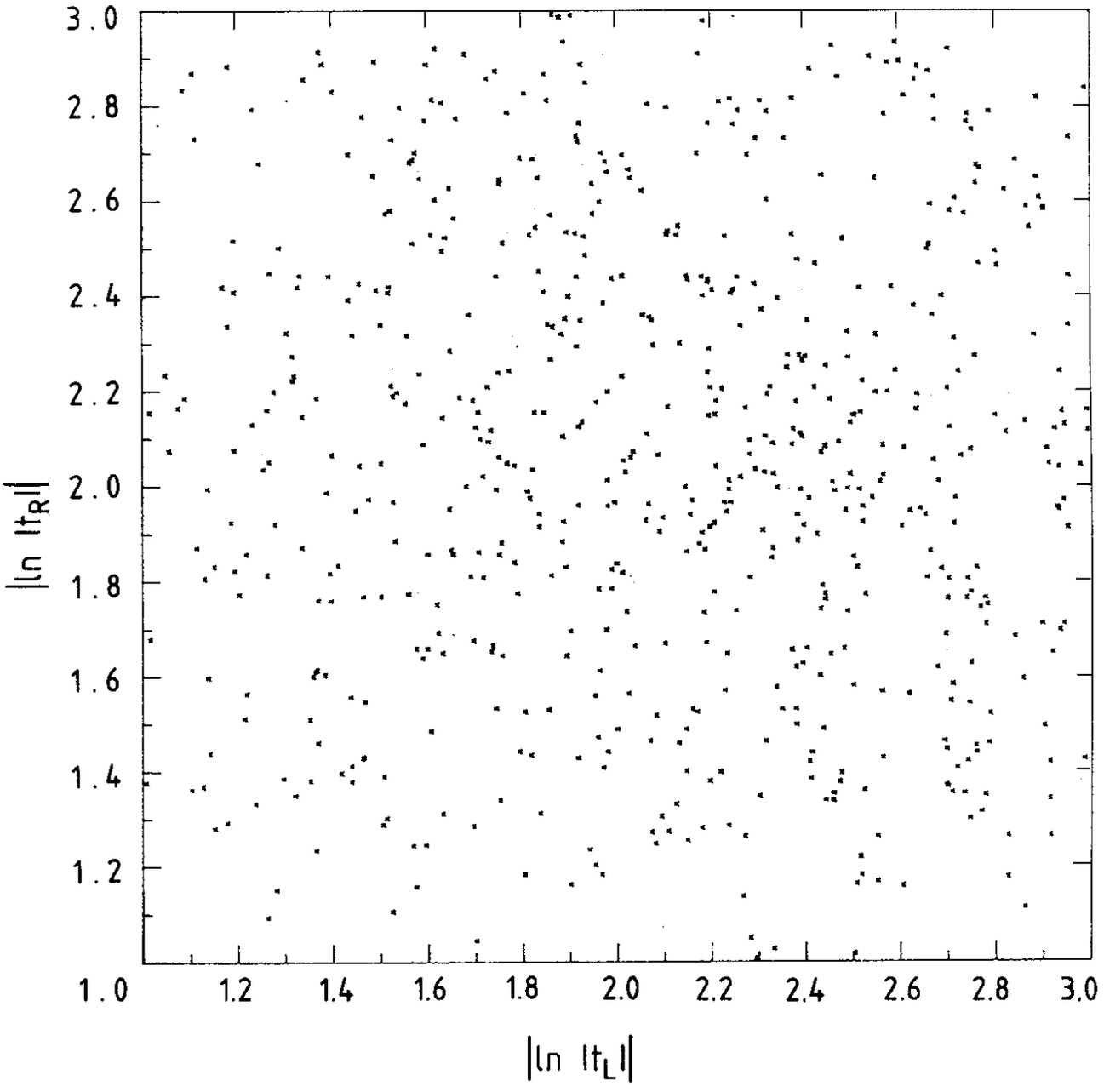
3.0
2.8
2.6
2.4
2.2
2.0
1.8
1.6
1.4
1.2
1.0
1.2
1.4
1.6
1.8
2.0
2.2
2.4
2.6
2.8
3.0
|ln |t_R||
|ln |t_L||

Fig. 3

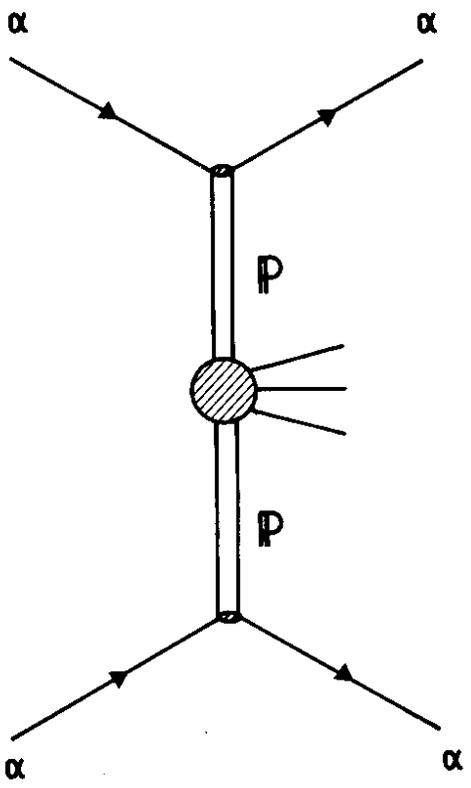

Fig. 4

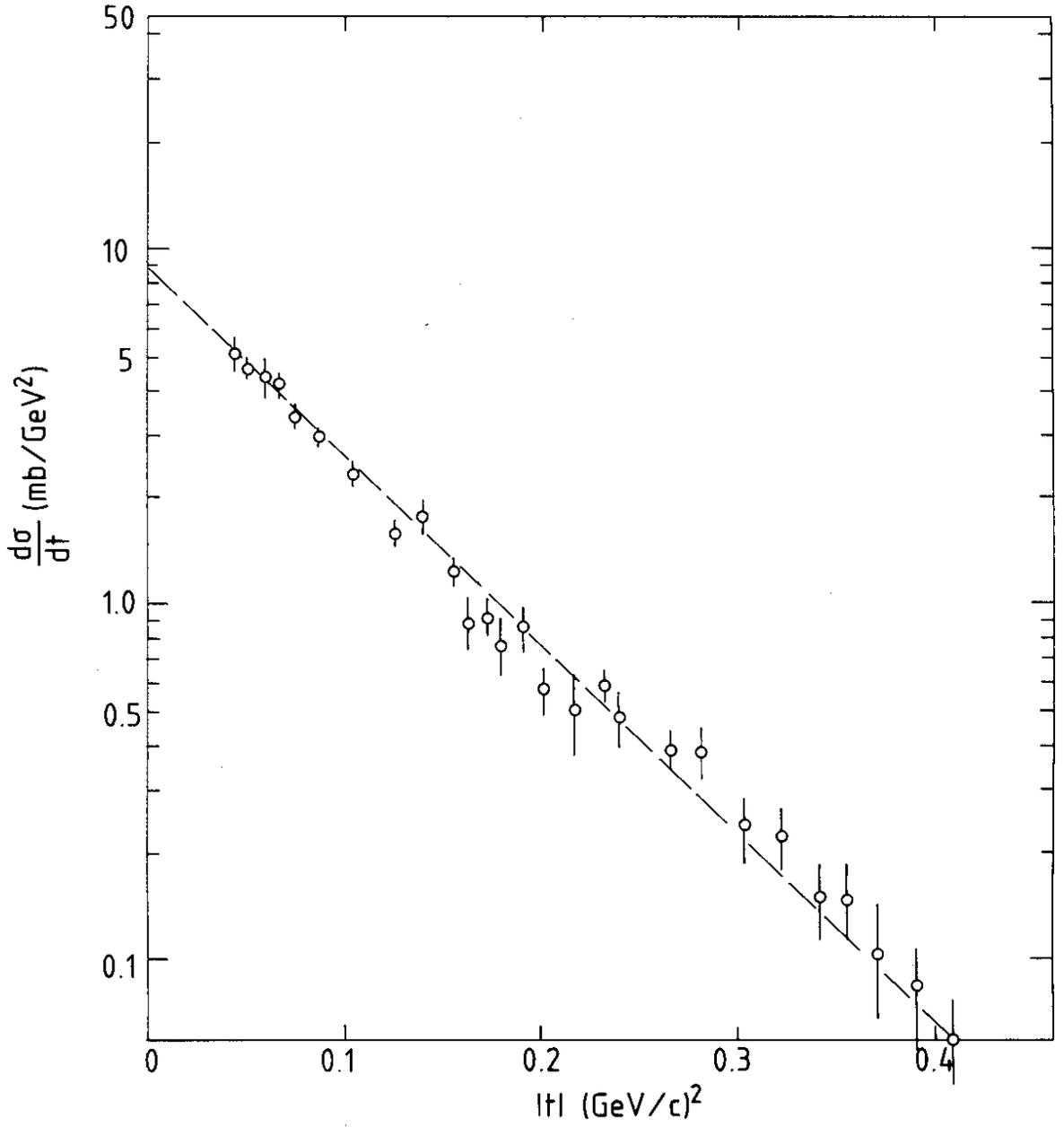

Fig. 5

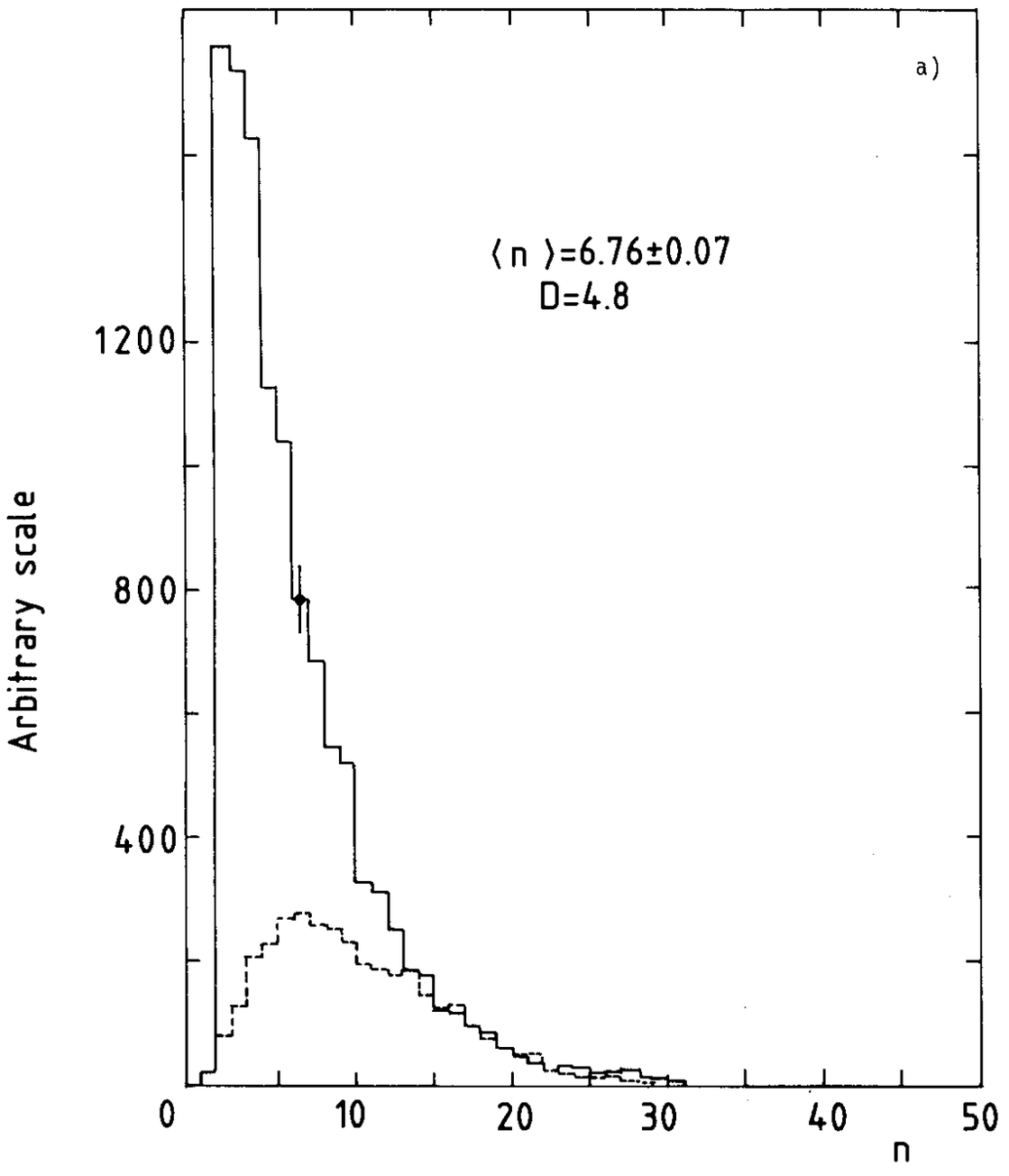

Fig. 6

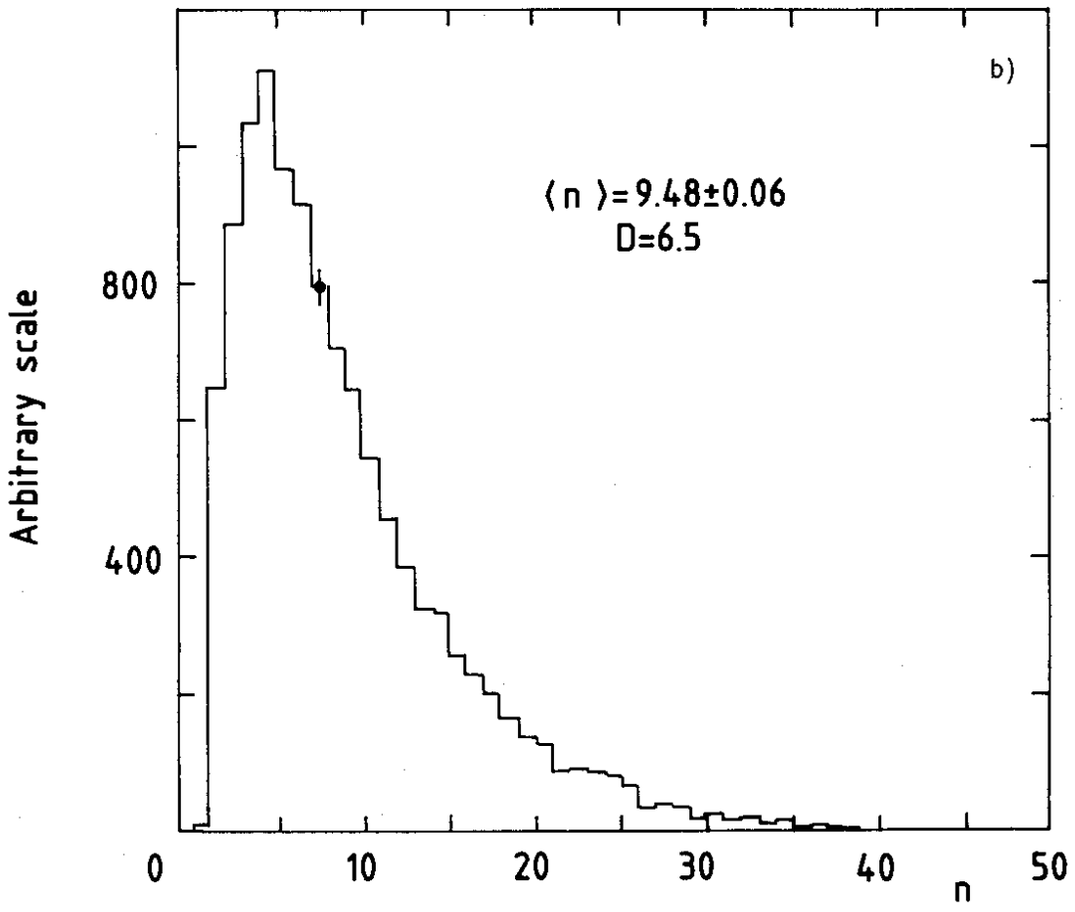

Fig. 6

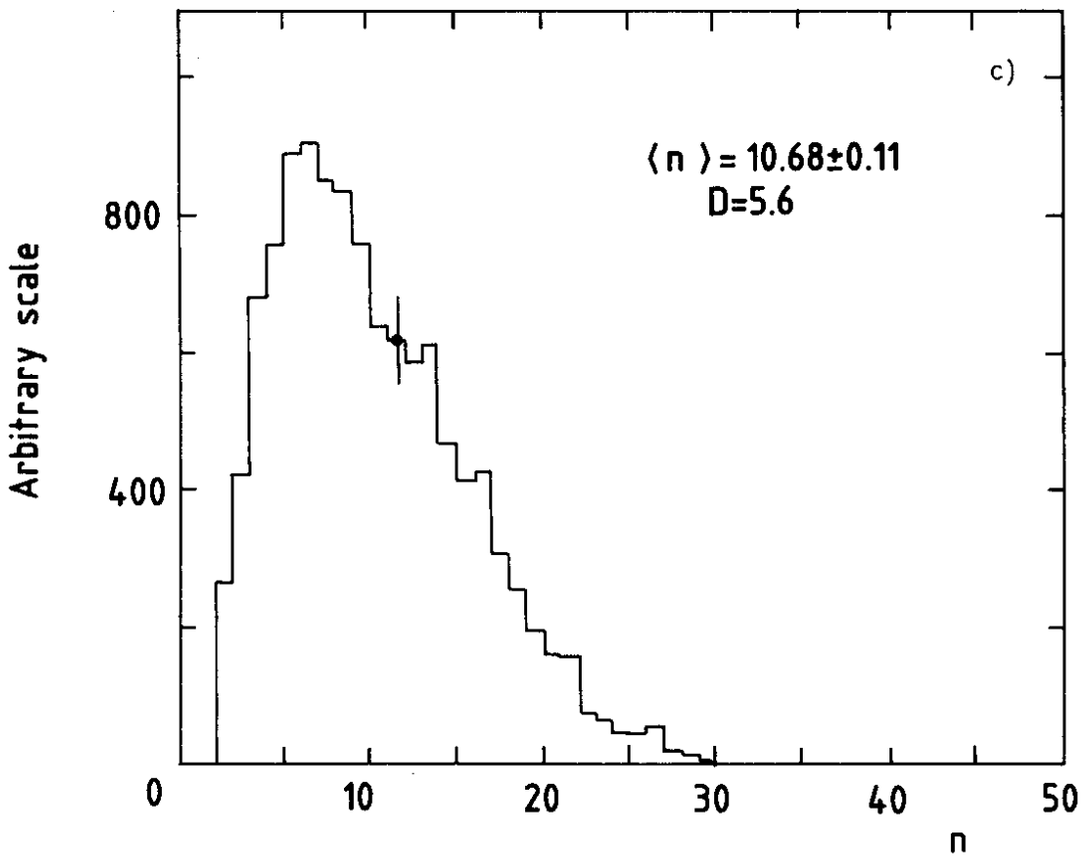

Fig. 6